



# An enhanced WDM optical communication system using a cascaded fiber Bragg grating

Ahmed F. Sayed<sup>1</sup> · Fathy M. Mustafa<sup>2</sup> · Ashraf A. M. Khalaf<sup>1</sup> · Moustafa H. Aly<sup>3</sup>

Received: 7 August 2019 / Accepted: 10 March 2020 / Published online: 14 March 2020  
© Springer Science+Business Media, LLC, part of Springer Nature 2020

## Abstract

In this paper, a cascaded fiber Bragg grating (FBG) system is proposed to reduce the dispersion in the optical signal in single mode optical fibers. This consequently enhances the system performance, which is evaluated by the bit error rate (BER) and quality factor (Q-factor). The proposed model consists of four uniform cascaded FBGs connected at the transmitter to get narrow linewidth,  $\Delta\lambda$ , of the optical signal, which is a major cause of the delay. The Optisystem7 is used to simulate the proposed model in a WDM system with and without the model for distance 200 km. The system parameters are investigated showing an enhanced performance with 12%, including eye diagram, Q-factor and BER. A  $10^{-6}$ – $10^{-10}$  BER is achieved with a quality factor in the range 7–14, including the effects of fiber length, input power and FBG length.

**Keywords** Fiber Bragg grating · Q-factor · Bit error rate · WDM system · Optisystem7

---

✉ Moustafa H. Aly  
mosaly@aast.edu; drmosaly@gmail.com

Ahmed F. Sayed  
ahmed.darwesh.te@gmail.com

Fathy M. Mustafa  
fmmg80@eng.bsu.edu.eg

Ashraf A. M. Khalaf  
ashkhalaf@yahoo.com

<sup>1</sup> Electronics and Communications Engineering Department, Faculty of Engineering, Minia University, Minya, Egypt

<sup>2</sup> Electrical Engineering Department, Faculty of Engineering, Beni-Suef University, Beni-Suef, Egypt

<sup>3</sup> Electronics and Communication Engineering Department, College of Engineering and Technology, Arab Academy for Science, Technology and Maritime Transport, P.O.B. 1029, Abou Kir, Alexandria, Egypt

## 1 Introduction

In the optical communication systems, when a range of wavelengths,  $\Delta\lambda$  is emitted from the light source, these wavelengths propagate along the optical fiber with different velocities and arrive the receiver at different times causing dispersion (Kaur et al. 2015; Venghaus and Grote 2017). The dispersion decreases the bit rates, signal to noise ratio and system performance (Agrawal 2012; Keiser 2000). To overcome this, many dispersion compensation techniques have been developed. The use of fiber Bragg grating (FBG) is one of the efficient tools used in dispersion compensation (Erdogan 1997; Mahmood 2018). The FBG is small part of an optical fiber having small different refractive indices planes inside its core. These planes are distributed in equal spaces in case of uniform FGB and unequal spaces in case of chirped fiber Bragg grating (CFBG) (Meena and Meena 2020; Meena and Gupta 2019). In the case of uniform FGB, the planes reflect a single wavelength with a certain bandwidth  $\Delta\lambda$  called Bragg wavelength and pass all other wavelengths (Daud and Ali 2018). In the case of CFBG, more wavelengths are reflected from different unequal distant planes, along the core, which gives it the ability to compensate dispersion (Sayed et al. 2017; Bhardwaj and Gaurav 2015). In (Srikar and Subhashini 2018) different types of dispersion compensation techniques are used in WDM Systems to minimize dispersion where the effect of using DCF and CFBG individually on the system performance are investigated. In (Ghosh and Priye 2018), dispersion compensation scheme is studied using four cascaded CFBGs to compensate the dispersion accumulated over 100 km of a conventional fiber, where a tanh apodization profile was used in CFBG. In (Joshi and Mehra 2016), a dispersion compensating fiber (DCF) is used with linear chirped apodized FBG.

The effect of input power, distance, and input bit rate is investigated. The system performance is analyzed in terms of eye-diagram, bit error rate (BER) and Q-factor. In (Panda et al. 2016), the use of CFBG have been discussed to compensate dispersion in WDM system. The simulation also optimized the power levels and CFBG length on the Q-factor and BER.

In this paper, we propose a unit that consists of four uniform cascaded FBGs connected to the transmitter to get a narrower full-width half maximum (FWHM) bandwidth,  $\Delta\lambda$  of the transmitted optical signal to reduce the propagation delay of the output signal in the optical fiber. This unit is first tested and verified through its reflectivity and FWHM. It is then connected to a WDM system and the system performance is evaluated through its eye-diagram, Q-factor and BER. Matlab is first used in verification and Optisystem7 is then used for simulation.

Our proposed system is unique because of its low power consumption compared to DCF, leading to a reduction in power budget and in system cost. It has a small size, where it can be used as a solution in the integrated optics with Mach–Zehnder in one chip and gives better results than DCF.

The remainder of this paper is organized as follows. The basic model and analysis are discussed in Sec. II. Section III illustrates the proposed system. Simulation results are displayed and discussed in Sec. IV. Section V is devoted to the main conclusions.

## 2 Basic model and analysis

Here, reflectivity equations are derived through a T-matrix formalism. Uniform FBG and CFBG are considered.

### 2.1 Uniform FBG

Figure 1 shows two counter-of an optical fiber, having a uniform FBG of length  $l$  and period  $\Lambda$  (Kashyap 1999).

Here,  $I_0$  and  $S_0$  are, respectively, the intensities of incident and reflected optical signals.  $I_1$  is the output (transmitted) optical signal and  $S_1$  is the reflected optical signal at the grating output and is set to zero.

The transfer matrix,  $T$ , for one FBG can be expressed as Venghaus (2006)

$$T = \begin{bmatrix} T_{11} & T_{12} \\ T_{21} & T_{22} \end{bmatrix} \tag{1}$$

The incident and reflected waves can be expressed by means of the T matrix as Venghaus (2006)

$$\begin{bmatrix} I_0 \\ S_0 \end{bmatrix} = \begin{bmatrix} T_{11} & T_{12} \\ T_{21} & T_{22} \end{bmatrix} \begin{bmatrix} I_1 \\ 0 \end{bmatrix} \tag{2}$$

where  $S_1$  is set to zero.

### 2.2 Chirped fiber Bragg grating

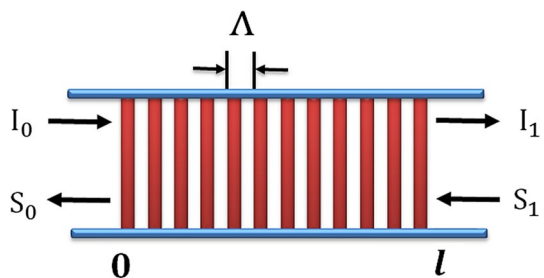
Now, the definition equations for CFBG are illustrated. The Bragg wavelength along the core of the CFBG,  $\lambda_B(z)$ , and the refractive index,  $n(z)$ , are given by Kashyap (1999), Ashry et al. (2014).

$$\lambda_B(z) = 2n(z)\Lambda(z) \tag{3}$$

and

$$n(z) = n_{eff} + \Delta n g(z) \cos \left\{ \frac{2\pi z}{\Lambda_0} (1 + xz) \right\} \tag{4}$$

Fig. 1 FBG section



where  $x$  is the linear chirp parameter (or slope) of the grating and  $g(z)$  is the apodization function (Mohammed et al. 2015, 2016). The spaces between planes along grating are Sayed et al. (2017).

$$\Lambda(z) = \Lambda_0 + xz \tag{5}$$

where  $\Lambda_0$  is the first space on the core.

The chirp,  $\Delta\lambda$ , between two ends of the grating is given by El-Gammal et al. (2015):

$$\Delta\lambda = 2n_{eff}(\Lambda_{long} - \Lambda_{short}) \tag{6}$$

where  $\Lambda_{long}$  is the longest period and  $\Lambda_{short}$  the shortest period inside the CFBG core.

The time delay,  $\tau$ , for each wavelength along the CFBG can be obtained by El-Gammal et al. (2015):

$$\tau(\lambda) = (\lambda_B - \lambda) \frac{2n_{eff}}{\Delta\lambda c} l \tag{7}$$

where  $c$  is the speed of light.

The dispersion parameter,  $D_g$ , of the CFBG can be obtained as Venghaus (2006):

$$D_g = \frac{2n_{eff}}{\Delta\lambda c} l \tag{8}$$

### 3 The proposed system

We start with the proposed model mathematical equation and its derivation. Then, simulation results of the proposed model are displayed through Optisystem7. The proposed model is then extended to the transmitter of a WDM network enhancing its performance.

#### 3.1 Model and analysis

The proposed model aims to achieve a narrower spectral width,  $\Delta\lambda$ , of the transmitted optical signal using cascaded uniform FBGs. It consists of four cascaded uniform FBGs. Figure 2 shows four identical cascaded FBGs, where the reflected signal of each stage is the input signal for the new stage. The reflectivity of each stage is derived related to the first stage. The normal parameters of the four identical uniform cascaded FBG with the most used frequency 193.1 THz are illustrated in the Table 1.

##### 3.1.1 First FBG stage

The parameters of the first stage are defined as  $I_{01}$ , the incident optical signal,  $S_{01}$  the reflected optical signal and  $I_{11}$  the output optical signal. The reflected optical signal at the output of the grating is set to zero. Therefore, following the procedure carried out above, the transfer matrix is defined as:

$$\begin{bmatrix} I_{01} \\ S_{01} \end{bmatrix} = \begin{bmatrix} T_{11} & T_{12} \\ T_{21} & T_{22} \end{bmatrix} \begin{bmatrix} I_1 \\ 0 \end{bmatrix} \tag{9}$$

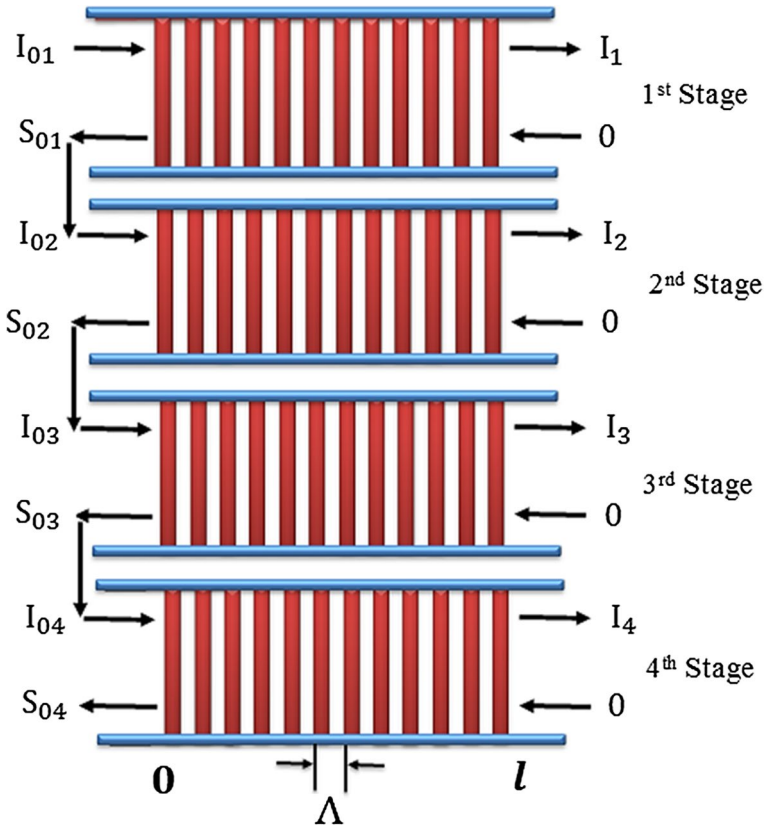


Fig. 2 Four cascaded FBGs

Table 1 FBG parameters

Parameter	Value
FBG grating length	2 mm
Frequency	193.1 THz
Effective refractive index	1.45
Induced refractive index	$8E-4$

So

$$I_{01} = T_{11}I_1 \tag{10}$$

$$S_{01} = T_{21}I_1 = \frac{I_{01}T_{21}}{T_{11}} \tag{11}$$

Then, reflectivity of the first stage,  $R_{01}$ , is obtained as

$$R_{01} = |\rho_{01}|^2 \quad (12)$$

where

$$\rho_{01} = \frac{S_{01}}{I_{01}} = \frac{T_{21}}{T_{11}} \quad (13)$$

### 3.1.2 Second FBG stage

In this case, the reflected optical signal of the first FBG is connected as the input signal of second FBG, which has the same T matrix of the first FBG. Following Fig. 2m the T matrix of the two FBG stages can be represented as

$$\begin{bmatrix} I_{02} \\ S_{02} \end{bmatrix} = \begin{bmatrix} T_{11} & T_{12} \\ T_{21} & T_{22} \end{bmatrix} \begin{bmatrix} I_2 \\ 0 \end{bmatrix} \quad (14)$$

In this case

$$S_{01} = I_{02} = I_{01} \frac{T_{21}}{T_{11}} \quad (15)$$

$$\begin{bmatrix} I_{01} \frac{T_{21}}{T_{11}} \\ S_{02} \end{bmatrix} = \begin{bmatrix} T_{11} & T_{12} \\ T_{21} & T_{22} \end{bmatrix} \begin{bmatrix} I_2 \\ 0 \end{bmatrix} \quad (16)$$

$$I_{01} \frac{T_{21}}{T_{11}} = T_{11} I_2 \quad (17)$$

Then,

$$I_{01} \frac{T_{21}}{T_{11}} = T_{11} I_2 \quad (18)$$

$$S_{02} = T_{21} I_2 \quad (19)$$

Hence, the reflectivity,  $R_{02}$ , for the second stage is

$$R_{02} = |\rho_{02}|^2 = \left| (\rho_{01})^2 \right|^2 = (R_{01})^2 \quad (20)$$

where

$$\rho_{02} = \frac{S_{02}}{I_{01}} = \left( \frac{T_{21}}{T_{11}} \right)^2 = (\rho_{01})^2 \quad (21)$$

### 3.1.3 Third FBG stage

In the same manner, and also following Fig. 2, we have

$$I_{03} = b_{02} = I_{01} \left( \frac{T_{21}}{T_{11}} \right)^2 \quad (22)$$

$$\begin{bmatrix} I_{01} \left( \frac{T_{21}}{T_{11}} \right)^2 \\ S_{03} \end{bmatrix} = \begin{bmatrix} T_{11} & T_{12} \\ T_{21} & T_{22} \end{bmatrix} \begin{bmatrix} I_3 \\ 0 \end{bmatrix} \quad (23)$$

$$I_{01} \left( \frac{T_{21}}{T_{11}} \right)^2 = T_{11} I_3 \quad (24)$$

$$I_{01} = \frac{(T_{11})^3}{(T_{21})^2} I_3 \quad (25)$$

$$S_{03} = T_{21} I_3 \quad (26)$$

Accordingly, the reflectivity,  $R_{03}$ , for the third FBG is

$$R_{03} = |\rho_{03}|^2 = |(\rho_{01})^3|^2 = (R_{01})^3 \quad (27)$$

where

$$\rho_{03} = \frac{S_{03}}{I_{01}} = \left( \frac{T_{21}}{T_{11}} \right)^3 \quad (28)$$

Similarly; for cascaded FBGs of the same parameters and each of a reflectivity  $R$ , the reflectivity of all  $n$  groups is equal  $(R)^n$ .

### 3.1.4 Fourth FBG stage

Following the same procedure, the reflectivity,  $R_{04}$ , is obtained as

$$R_{04} = (R_{01})^4 \quad (29)$$

## 3.2 Optisystem simulation of the proposed model

The simulation of the proposed model by Optisystem7 is illustrated in Fig. 3. The model has four stages.

As shown, the model consists of four cascaded stages of uniform FBGs, where the output of each stage is connected to the input of the next stage. A photonic parameter analyzer is connected to the input of the first stage. The output of the last stage is

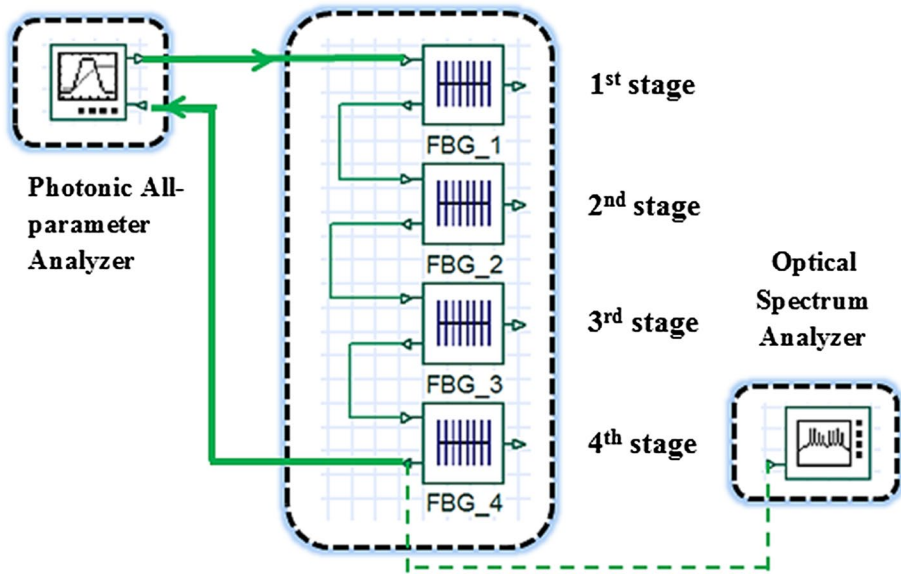


Fig. 3 Optisystem7 simulation of cascaded uniform FBG connection

connected to an optical spectrum analyzer to show the reflective wavelength bandwidth of the last stage and its power. The physical explanation is shown Fig. 2, where the reflected signal of each stage is the input signal for the new stage.

### 3.3 Optisystem simulation of the WDM system with enhanced performance

Here, we illustrate the simulated WDM system and its components. To enhance the WDM system performance, three cases are to be investigated. Case one is the WDM system without the proposed model. Case two is the connection of the proposed model between the laser source and the Mach–Zehnder at the transmitter in the WDM system. Case three is the connection of the proposed model between the Mach–Zehnder and the optical fiber.

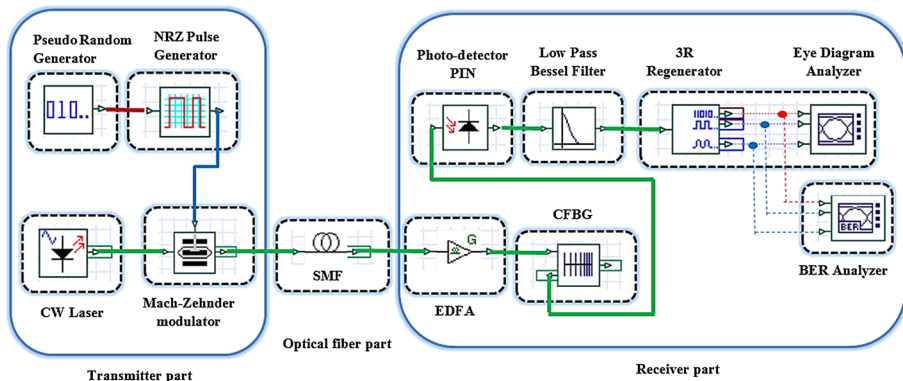


Fig. 4 Case one: simulated link with the proposed model before Mach–Zehnder modulator



**Table 2** CFBG parameters

Parameter	Value
CFBG grating length	80 mm
Frequency	193.1 THz
Effective refractive index	1.47
Induced refractive index	5E-5

**Table 3** WDM system parameters

Parameter	Value
Input power (dBm)	+ 5
Dispersion (ps/nm.km)	17
Bit rate(Gbps)	10
Attenuation (dB/km)	0.2
Fiber length (km)	200
EDFA gain (dB) with noise figure 4 dB	40
PIN photodetector with responsivity (A/W)	1
PIN photodetector with dark current (nA)	10
Bessel filter cut off frequency	0.75 × bit rate

### 3.3.1 Case one

Figure 4 shows the simulated WDM system without the proposed model. It consists of transmitter, fiber, and receiver. The transmitter consists of a data source, NRZ modulator driver, laser source and Mach–Zehnder modulator. The data source generates a pseudo-random bit sequence at a rate of 10 Gbps. The output of the data source is connected to the modulator driver which produces NRZ format pulses with a duty cycle of 0.5. The NRZ pulse generator converts the binary data into the electrical pulses that modulate the laser signal through the Mach–Zehnder modulator. The output of laser source is a continuous-wave type with a frequency of 193.1 THz ( $\lambda = 1553.6$  nm) and an output power of 5 dBm. The Mach–Zehnder modulator has an extinction ratio of 30 dB.

The optical fiber is of 200 km length and 17 ps/nm.km dispersion parameter and 0.2 dB/km attenuation coefficient. At the receiver part, the received signal is amplified by an erbium doped fiber amplifier (EDFA) with 40 dB gain and 4 dB noise figure to compensate the losses of the signal in the optical fiber. EDFA is operated at pump wavelength 980 nm and 100 mw pump power (Agrawal 2012). The dispersion compensator CFBG compensates the dispersion in the optical signal. The PIN photodetector has 1 A/W responsivity 10 nA dark current 10 nA to convert the optical signal into electrical. This is followed by a low pass Bessel filter which of cut off frequency equal to  $0.75 \times \text{bit rate}$  to filter the output signal. The optical regeneration (re-amplifying, re-shaping, and re-timing) is then used to restore the transmission impairments stemming from fiber chromatic dispersion and other nonlinearities which are connected to the eye diagram analyzer to draw the eye diagram and calculate BER for the WDM link. Table 2 shows the CFBG parameters used for dispersion compensation where the CFBG length is 80 mm (Kaur et al. 2015) and Effective refractive index is 1.47 (Sayed et al. 2017). Table 3 shows the WDM system parameters.

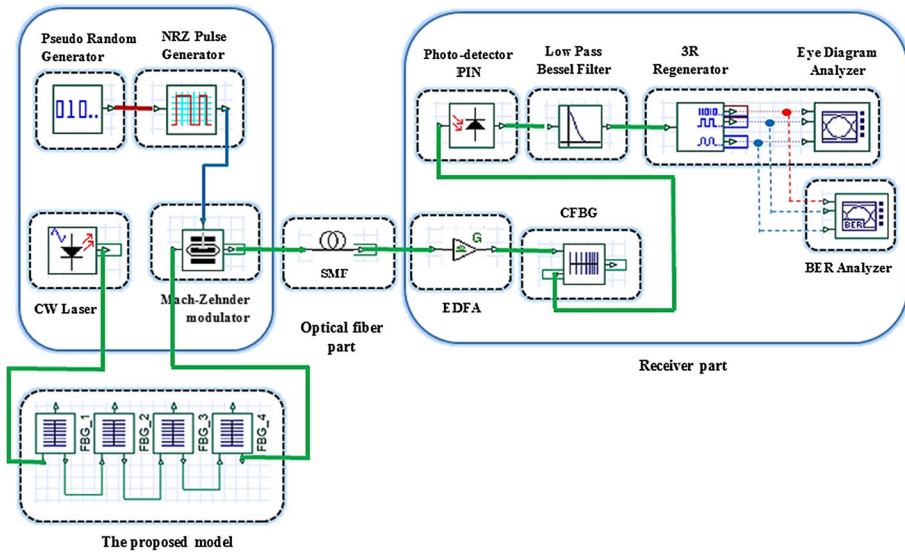


Fig. 5 Connection of the proposed model in case two

### 3.3.2 Case two

Figure 5 shows the connection of the proposed model in the WDM system. In this case, the connection of the proposed model is between the laser source and the Mach-Zehnder modulator at the transmitter of the WDM system.

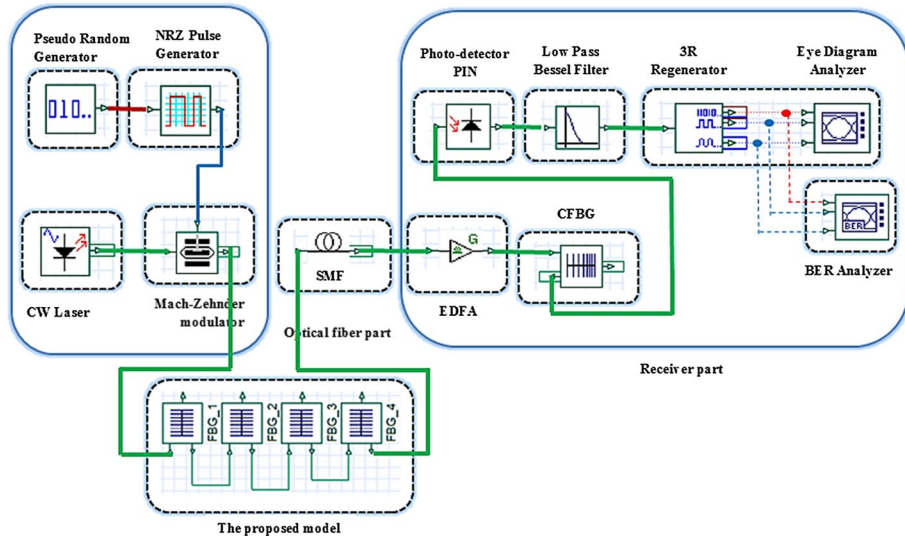


Fig. 6 Connection of the proposed model in case three

### 3.3.3 Case three

Figure 6 shows the connection of the proposed model between the Mach–Zehnder modulator and the optical fiber at the transmitter in the WDM system.

## 4 Simulation results and discussion

The proposed model mathematical equations are solved by Matlab, while the proposed model structure is simulated by Optisystem7. The validity of the proposed model is tested by comparing the reflectivity results of the FBG from the last stage with Matlab and with Optisystem7 in the three cases of the WDM system.

### 4.1 A comparative study for the three cases

It is noted that: (1) the FWHM,  $\Delta\lambda$ , gets narrower as the number of stages increases, (2) when increasing the number of stages, the maximum reflectivity decreases slightly and side lobes start to disappear. In Fig. 7b, where the reflected power from the last stage is proportional to the reflectivity, it acts as the same scenarios as in Fig. 7a. A fair agreement is noticed between analytical and simulation results in Fig. 7a and b assuring the validation of the proposed model. The comparison between the three cases includes the eye diagram, Q-factor, BER and BER contour patterns as follows. Figure 7a shows the results of the reflectivity from the last stage by Matlab.

The reflectivity of each stage is shown in the Fig. 7. Clearly, the reflectivity of the first stage is in blue, the second is red, the third is green and the fourth is black. As the number of stage increases, the bandwidth is reduced and also the side lobes, leading to a better performance.

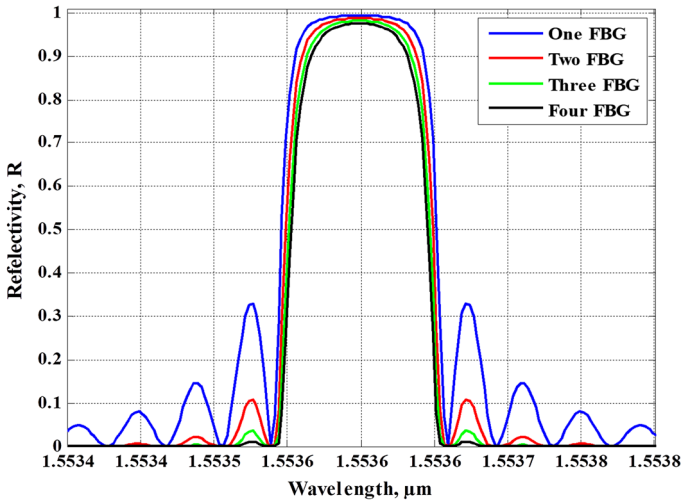
### 4.2 Eye diagram

Figure 8 shows the eye diagram of each case. The red curves represent eye diagram opening. Clearly, the largest one (1.514 mm) corresponds to case three, then case one and case two with heights 1.403 mm and 1.328 mm, respectively.

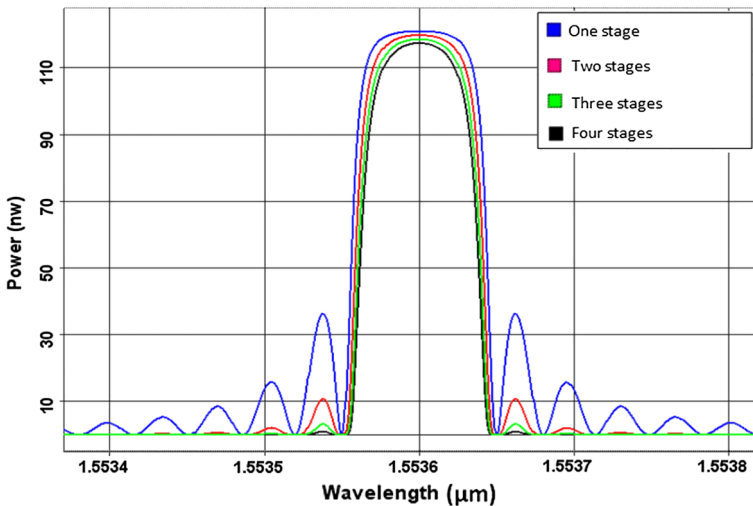
### 4.3 Q-factor

Figure 9 displays the relation Q-factor against the bit period for the three cases. It is noted that case three is the best one followed by cases one and two, respectively. This shows and confirms the use of our proposed model.

Now, we investigate the effect of input power, fiber length, and grating length in case three, on the Q-factor. Figure 10 shows that the Q-factor increases significantly with the input power reaching a maximum value of 14 at input power 14 dBm. To avoid nonlinear effects, we stopped calculations at 20 dBm, where the Q-factor reaches 8. Figure 11 shows that the Q-factor is gradually increasing until fiber length 70 km. After that, it is sharply increased to a peak of 20 at 120 km of fiber length. Next, it starts to decrease and reaches zero for at a fiber length  $\geq 240$  km. Figure 12 displays the dependence of the



(a) Reflectivity using Matlab.



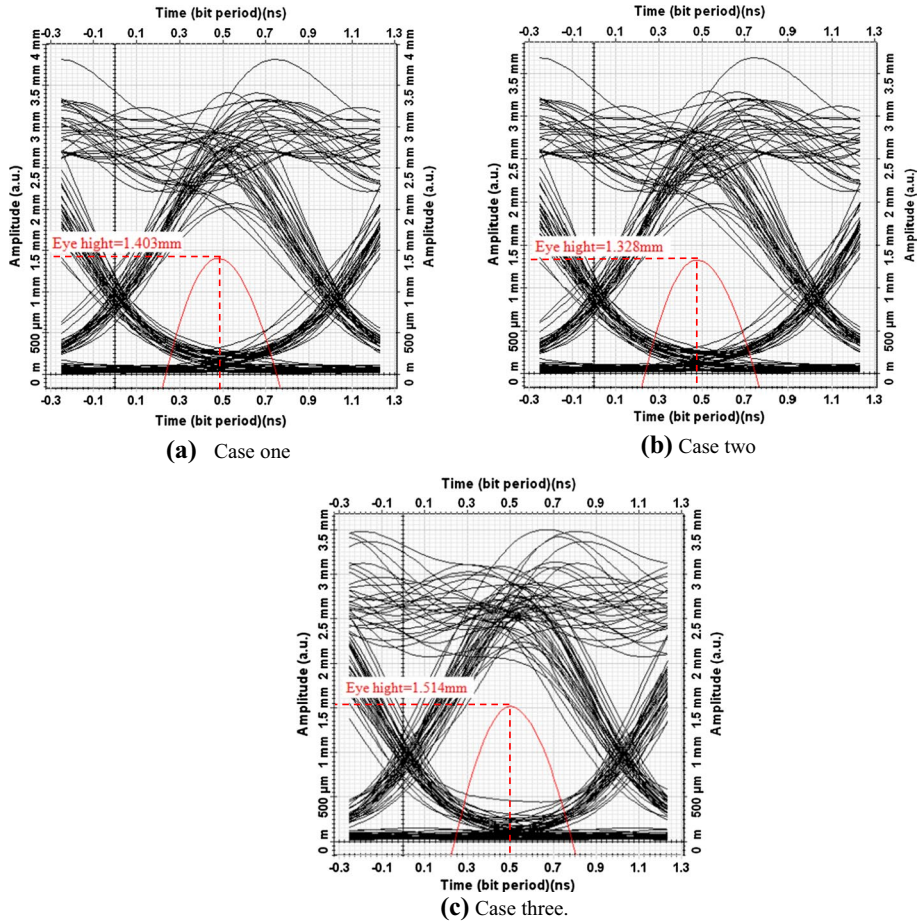
(b) Reflectivity using Optisystem7.

Fig. 7 Reflectivity using Matlab and Optisystem7

Q-factor on the grating length. Clearly, a grating length 110 mm achieves the best value of Q-factor.

As the length of FBG at the transmitter is longer, the reflectivity reaches to maximum and the bandwidth is reduced. The FWHM (Full Width Have Maximum) for  $\Delta\lambda$  reaches to minimum and reduces the delay at receiver. The dispersion compensation process by CFBG at receiver becomes easier that enhances the receiver performance.

Figure 13 shows the relation between the power (dBm) and the wavelength (μm) of the injected optical signal into the optical fiber. Obviously, our model in case three gives the narrower bandwidth for the optical signal injected to the fiber, leading to a better Q-factor.



**Fig. 8** Eye diagram the three cases

Another optimization has been done to get the best parameters to improve the quality factor is the relation between the Q-factor and the wavelength range in C band, in each case.

In cases one and two, Figs. 14 and 15, the Q-factor is sharply increasing to a peak of 8.54, and 8.4, respectively. The rest of the values fluctuate at level 7.3 and below 6.8, respectively. But, in case three, Fig. 16, the same behavior of Q-factor is achieved with a highest value of 8.68. Also, due to the enhanced Q-factor, new intermediate wavelengths have been appeared with peak values of Q-factor of 7.7 and 8 where have not appeared before in the other two cases. This ensures the superior performance of case three.

To require the betterment of optimization level, many parameters have been optimized in case three with the quality factor in the previous section such as: input power in Fig. 10, optical fiber length in Fig. 11, CFBG length in Fig. 12 and finally the wavelength in Fig. 16. To have an optimized WDM system with best performance with highest Q-factor, we should combine all these parameters together. From these figures, we have the optimum values as follows: input power is 14 dB, optical fiber length is

Fig. 9 Q-factor comparison

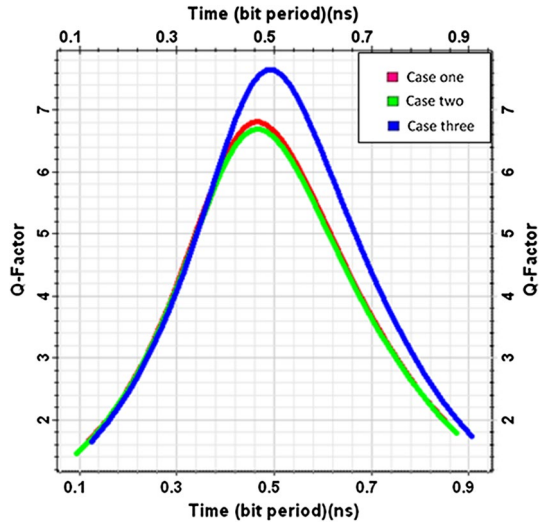


Fig. 10 Effect of input power on the Q-factor

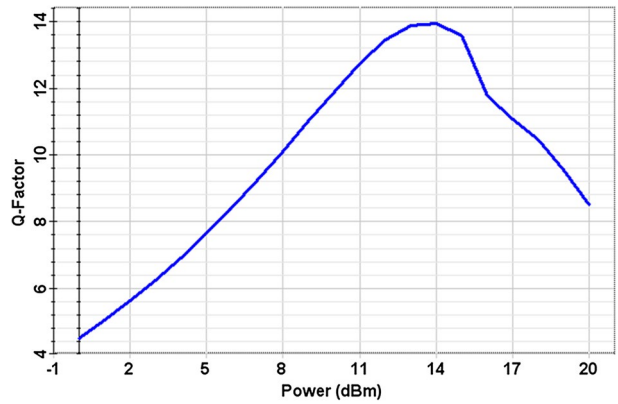
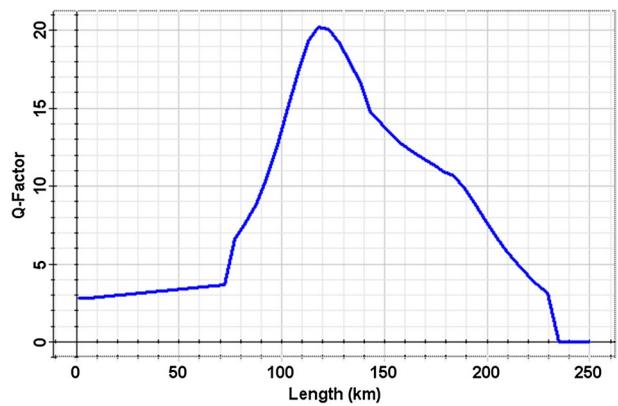
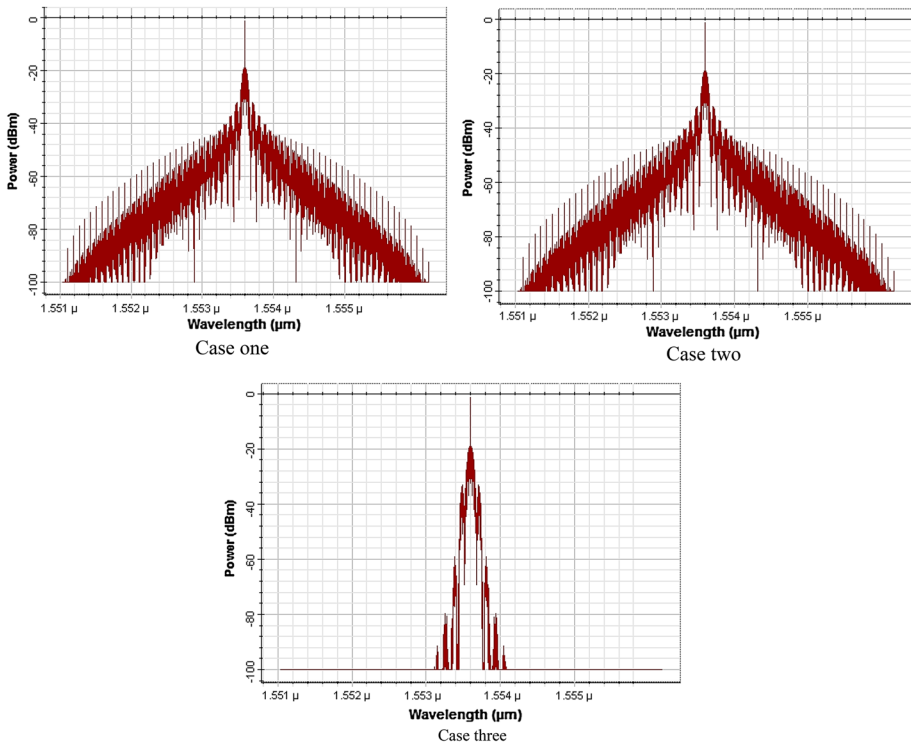
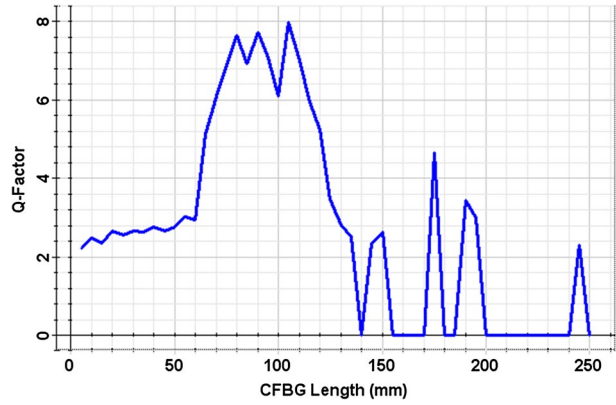


Fig. 11 Effect of fiber length on the Q-factor



**Fig. 12** Effect of FBG length on the Q-factor



**Fig. 13** Power versus wavelength for the three case

190 km, CFBG length with cost saving and 75 mm, at a wavelength of 1553.3 nm. Using these specific values, the whole WDM system in case three has been re-simulated with the chosen parameters, where it achieves 19.4 Q-factor.

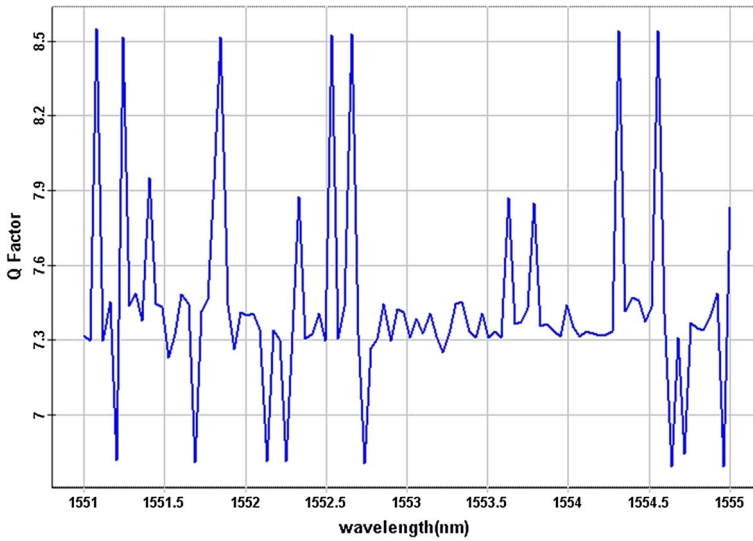


Fig. 14 Q-factor versus wavelength, Case one

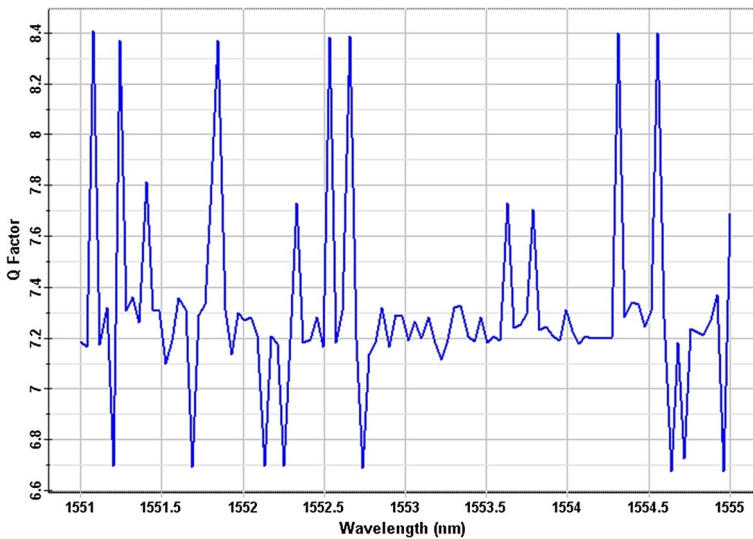


Fig. 15 Q-factor versus wavelength, Case two

#### 4.4 BER

A comparison between the three cases for the BER is shown in Fig. 17, against the bit period. Again, case three shows the best performance (least BER), followed by cases one and two, respectively. This shows and confirms the use of our proposed model.

The BER for proposed system is compared to Nokia 1830 Pss-16, Pss-32 DWDM multiplexer manual which states that: “The OT port has detected Excessive BER on



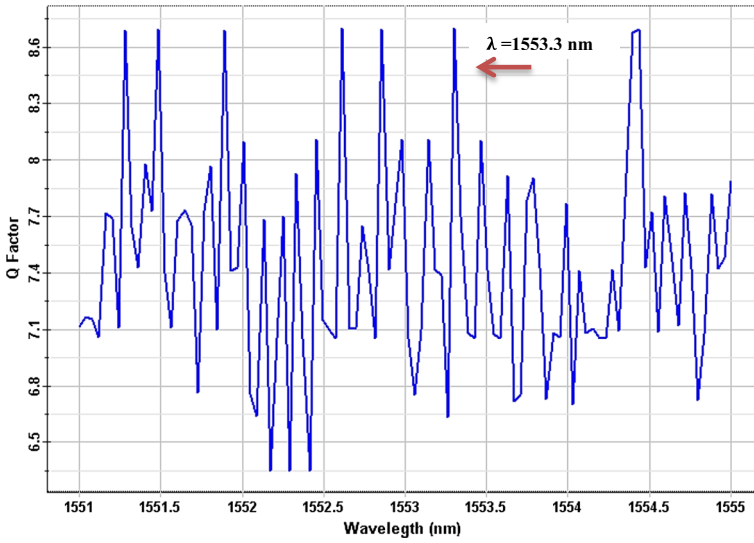
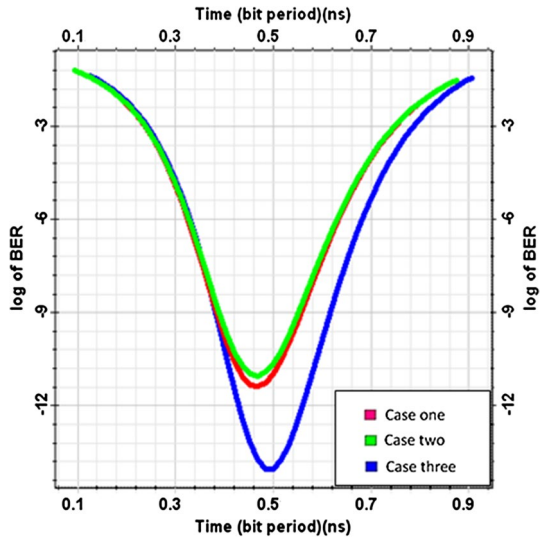


Fig. 16 Q-factor versus wavelength, Case three

Fig. 17 BER performance for the three cases



the OC-n/STM-n port of the 11STAR1 card. This defect indicates that a local OC-n/STM-n port has detected a BER that exceeds selected threshold. The default value is  $10^{-6}$  for STM-64 (also from STM-16, STM-4, STM-1), and  $10^{-7}$  for STM-256.” (Nokia 2020). The obtained results are also in a fair agreement with that stated by Huawei OSN 8800 T32 which stated that for 10G NRZ & (FEC) is lower than  $10^{-6}$  (Huawei 2020).

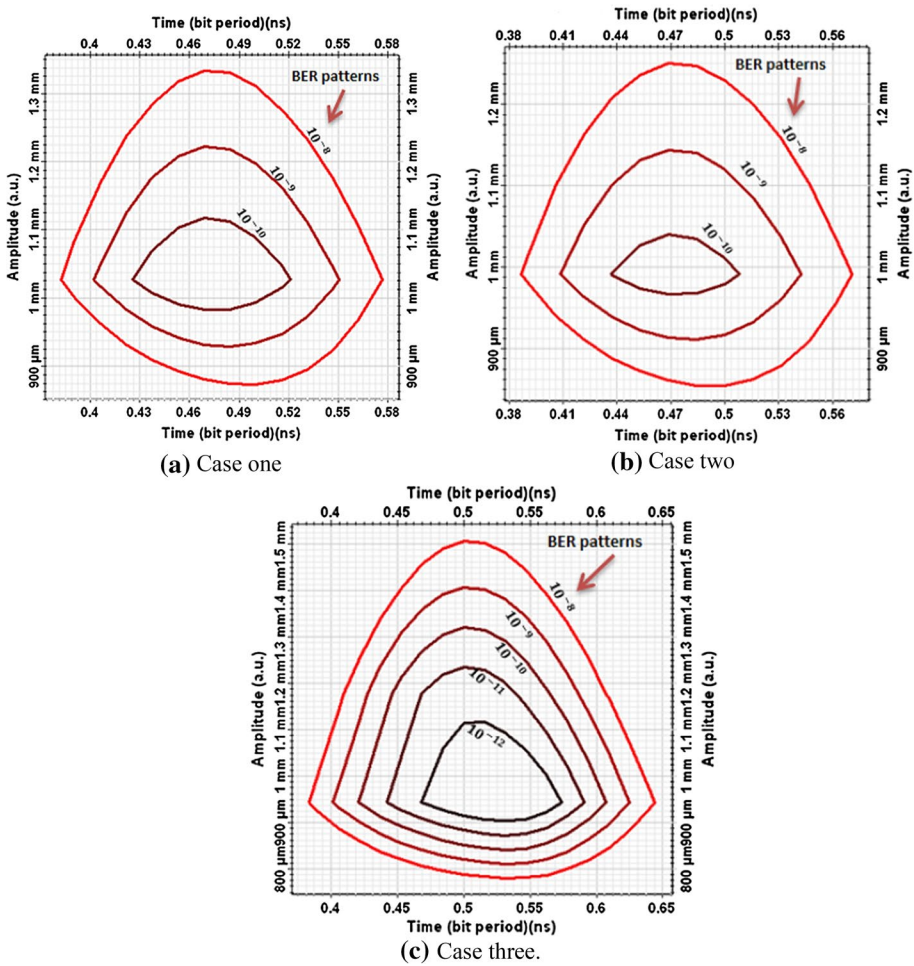


Fig. 18 BER contours for the three cases

### 4.5 BER contours

There are infrequently occurring events that are not visible in eye-diagram. So, multiple eye contours correspond to different BER levels showing the lowest level of BER. The BER contour line is an accurate method to measure the performance it shows all BER in the eye diagram lines. A comparison for the different cases is illustrated in Fig. 18. It shows the relation

**Table 4** Results comparison for each case

Cases	Without	With the proposed model	
	Case one	Case two	Case three
Q-factor	6.8	6.68	7.64
BER	5.26E-12	1.2E-11	1.096E-14

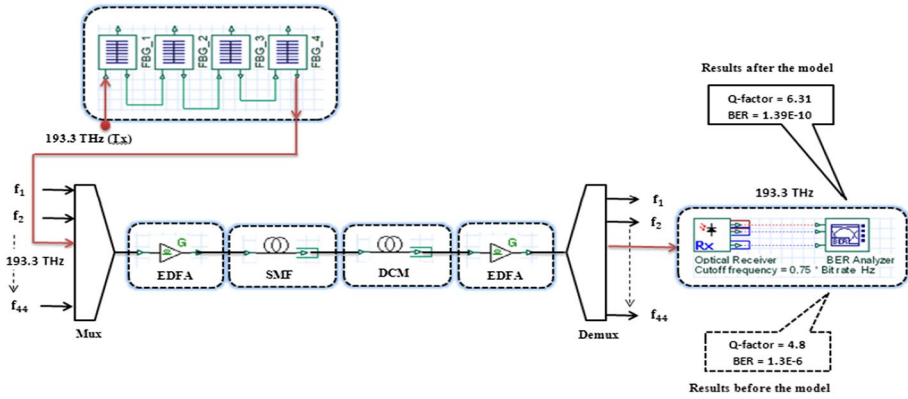


Fig. 19 Case study of a WDM link with Optisystem7

between the BER contour lines (mm) and the bit period (ns). From comparison, it is found that case three gives the better BER, where the contour lines are constructed from  $1E-8$  to  $1E-12$  BER. In other cases (a) case two and (b) case three, it counts only from  $1E-8$  to  $1E-10$  BER.

Table 4 summarizes the performance evaluation parameters in a useful comparison. The results show that case three is the best one, where the connection of the proposed model between the Mach–Zehnder modulator and the optical fiber at the transmitter in the WDM system.

### 4.6 WDM link

A WDM link is designed using our proposed as shown in Fig. 19. It consists of 44 individual channels connected to the multiplexer to multiplex them together as a one group channels. EDFA with a gain 10 dB acts as a pre-amplifier to amplify channels before transmission. The fiber used is a single mode fiber with 11.8 km length which carries the multiplexed channels to the receiver part. In the receiver, a DCM with length 1 km compensates the dispersion of the 44 channels. A post amplifier EDFA with a gain 7 dB amplifies the optical channels to compensate the attenuation in the optical fiber. The de-multiplexer is used to demultiplex the channels from EDFA. The frequency channel 193.3 THz is connected to the receiver with a band pass filter of a cut off frequency  $0.75 \times \text{bit rate}$ . The BER analyzer calculates the Q-factor and BER for the channel frequency 193.3 THz.

The obtained results are displayed in Fig. 20. A comparison for both Q-factor and BER before and after using our proposed model. The system gives results for Q-factor 4.8 and  $1.3E-6$  for BER at 193.3 THz. After applying the proposed model at transmitter as shown in Fig. 19, both Q-factor and BER are improved to 6.31 and  $1.39E-10$ , respectively. It is shown an appreciable improvement in both Q-factor and BER when applying our proposal. Table 5 summarizes this comparison.

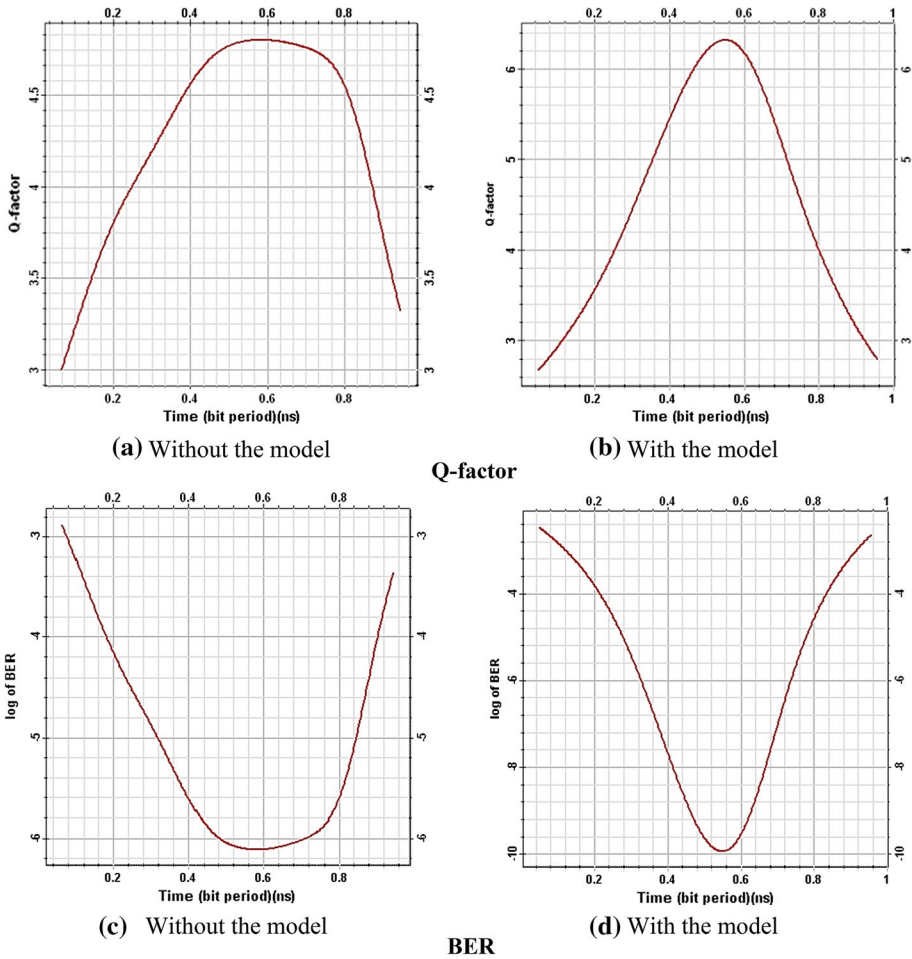


Fig. 20 Q-factor and BER without and with applying the proposed model

Table 5 Enhanced WDM system using our proposed mode

Parameter	Without the model	With the model
Q-factor	4.8	6.31
BER	$1.3\text{E}-6$	$1.39\text{E}-10$

### 5 Conclusion

In this paper, we proposed a cascaded FBG system that aims to reduce the used spectral width of the transmitted optical signal to reduce the propagation delay and improve system performance. The proposed model mathematical equations are simulated with Matlab and the proposed model structure is simulated by Optisystem7. A WDM system is simulated at distance 200 km with three cases. It is found that when the proposed cascaded FBG system

is connected between Mach-Zhender modulator and the optical fiber. This connection appreciably enhanced the system performance parameters including eye diagram, Q-factor, and BER. A Q-factor of 7.94 and a BER of  $1.96E-14$  are achieved.

## References

- Agrawal, G.P.: *Fiber-optic Communication Systems*. Wiley, New York (2012)
- Ashry, I., Elrashidi, A., Mahros, A., Alhaddad, M., Elleithy, K.: Investigating the performance of apodized fiber Bragg gratings for sensing applications. In: *Proceeding of the Conference of the American Society for Engineering Education*, Bridgeport, Connecticut, USA, Vol. 14, pp. 1–5, 3–5 (2014)
- Bhardwaj, A., Gaurav, S.: Performance analysis of 20 Gbps optical transmission system using fiber Bragg grating. *Int. J. Sci. Res. Publ.* **5**(1), 1–4 (2015)
- Daud, S., Ali, J.: *Fibre Bragg Grating and No-Core Fibre Sensors*. Springer, New York (2018)
- El-Gammal, H.M., Fayed, H.A., El-Aziz, A.A., Aly, M.H.: Performance analysis & comparative study of uniform, apodized and pi-phase shifted FBGs for array of high performance temperature sensors. *Optoelectron. Adv. Mater. Rapid Commun.* **9**(9–10), 1251–1259 (2015)
- Erdogan, T.: Fiber grating spectra. *J. Lightwave Technol.* **15**(8), 1277–1294 (1997)
- Ghosh, C., Priye, V.: Dispersion compensation in a  $24 \times 20$  Gbps DWDM system by cascaded chirped FBGs. *Optik* **164**, 335–344 (2018)
- Huawei. <https://support.huawei.com/carrier/docview!docview?nid=DOC1000156388&path=PBI1-7275726/PBI1-7275738/PBI1-7275807/PBI1-22318901/PBI1-16323/PBI1-20369/PBI21336524/PBI1-21336526>, 2020
- Joshi, V., Mehra, R.: Performance analysis of an optical system using dispersion compensation fiber & linearly chirped apodized fiber Bragg grating. *Open Phys. J.* **3**(1), 114–121 (2016)
- Kashyap, R.: *Fiber Bragg Gratings*. Academic Press, New York (1999)
- Kaur, M., Sarangal, H., Bagga, P.: Dispersion compensation with dispersion compensating fibers (DCF). *Int. J. Adv. Res. Comput. Commun. Eng.* **4**(2), 354–356 (2015)
- Keiser, R.: *Signal Degradation in Optical Fibers*. McGraw-Hill, New York (2000)
- Mahmood, A.: DCF with FBG for dispersion compensation in optical fiber link at various bit rates using duobinary modulation format. *Eng. Technol. J.* **36**(5), 514–519 (2018)
- Meena, M.L., Gupta, R.K.: Design and comparative performance evaluation of chirped FBG dispersion compensation with DCF technique for DWDM optical transmission systems. *Optik* **188**, 212–224 (2019)
- Meena, D., Meena, M.L.: Design and Analysis of Novel Dispersion Compensating Model with Chirp Fiber Bragg Grating for Long-Haul Transmission System. *Optical and Wireless Technologies*. Springer, Singapore, pp. 29–36 (2020)
- Mohammed, N.A., Elashmawy, A.W., Aly, M.H.: Distributed feedback fiber filter based on apodized fiber Bragg grating. *Optoelectron. Adv. Mater. Rapid Commun.* **9**(9–10), 1093–1099 (2015)
- Mohammed, N.A., Okasha, N.M., Aly, M.H.: A wideband apodized FBG dispersion compensator in long haul WDM systems. *J. Optoelectron. Adv. Mater.* **18**(5–6), 475–479 (2016)
- Nokia. <https://www.manualslib.com/download/1350537/Alcatel-Lucent-1830-Pss-16.html>, 2020
- Panda, T.K., Sahu, A.N., Sinha, A.: Performance analysis of 50 km long fiber optic link using fiber bragg grating for dispersion compensation. *Int. Res. J. Eng. Technol.* **3**(3), 95–98 (2016)
- Sayed, A.F., Barakat, T.M., Ali, I.A.: A novel dispersion compensation model using an efficient CFBG reflectors for WDM optical networks. *Int. J. Microw. Opt. Technol.* **12**(3), 230–238 (2017)
- Srikar, S.S.S., Subhashini, N.: Analysis of dispersion compensation methods in WDM systems. In: *Optical and Microwave Technologies*. Springer, Singapore, pp. 269–278 (2018)
- Venghaus, H.: *Wavelength Filters in Fiber Optics*. Springer, Berlin (2006)
- Venghaus, H., Grote, N.: *Fibre Optic Communication*. Springer International Publishing, Cham (2017)

**Publisher's Note** Springer Nature remains neutral with regard to jurisdictional claims in published maps and institutional affiliations.